






Article

# Zero power mismatch islanding detection algorithm for hybrid distributed generating system

Sareddy Venkata Rami Reddy<sup>1</sup>, T. R. Premila<sup>1</sup>, Ch. Rami Reddy<sup>2,\*</sup>, and B. Nagi Reddy<sup>3,\*</sup>

<sup>1</sup> Department of Electrical and Electronics Engineering, Vels Institute of Science, Technology & Advanced Studies, Pallavaram, Chennai, 600117, India

<sup>2</sup> Department of Electrical and Electronics Engineering, Joginpally B R Engineering College, Hyderabad, 500075, India

<sup>3</sup> Department of Electrical and Electronics Engineering, Vignana Bharathi Institute of Technology, Hyderabad 501301, India

\* Correspondence: creddy229@gmail.com, nagireddy208@gmail.com

Received: 08 July 2023; Accepted: 28 August 2023; Published: 04 October 2023

**Abstract:** Distributed generation is essential for both keeping up with the rising power demand and reducing the amount of money spent on fossil fuels. There is widespread agreement that the world should prioritize the development of renewable energy systems such as wind and solar energy. This study describes the design and utility-grid integration of a hybrid distributed generating system that utilizes photovoltaic and wind-driven permanent magnet synchronous generators (hybrid PMSG-PV systems). To prevent damage to the grid, hybrid distributed generation systems, consumer devices, and line workers must be protected from islanding. Detection of islanding in hybrid DG systems has been suggested using passive islanding and time-spectral analysis. Measuring and amplifying the ripple content present in voltage at point of common coupling (PCC) about 0.4 seconds after the permissible delay time after the circuit breaker opens on the utility grid side is how islanding is discovered using this method. Compared to other methods, the proposed method has smoother islanding detection waveforms owing to increases in both the window size and threshold limit. The suggested method detects islanding in 40 ms and is verified in a variety of non-islanding scenarios, such as fault occurrence, parallel feeder loss, and load shift. In addition, the cost is reduced, the response time is rapid, and there is no non-detection zone (NDZ) when using these methods. Unlike active islanding detection methods, their function is unaffected by the size, quantity, or type of distributed generators linked to the utility grid; hence, there are no power quality concerns.

© 2023 by the authors. Published by Universidad Tecnológica de Bolívar under the terms of the [Creative Commons Attribution 4.0 License](https://creativecommons.org/licenses/by/4.0/). Further distribution of this work must maintain attribution to the author(s) and the published article's title, journal citation, and DOI. <https://doi.org/10.32397/tesea.vol4.n2.534>

## 1. Introduction

Generation prices for renewable energy like wind and solar photovoltaic (PV) have dropped significantly during the past few years. This has led to some improvement in the actual number of privately funded wind

**How to cite this article:** Sareddy Venkata Rami Reddy, T R Premila, Ch Rami Reddy, and B Nagi Reddy. Zero power mismatch islanding detection algorithm for hybrid distributed generating system. *Transactions on Energy Systems and Engineering Applications*, 4(2): 534, 2023. DOI:10.32397/tesea.vol4.n2.534

and solar generating plants [1]. Unintentional electrical islanding poses a greater threat to the distributed generation units that are integrating with the utility grid and must be prevented [2]. Part of the electrical energy network is isolated from the remaining portion of the utility grid and is continually energized by a distributed generation (DG) unit, as specified by IEEE standard 929-2000. To prevent damage to DG and electrical equipment connected to the utility network, the parameters, voltage, and frequency, must be strictly limited at all times [3]. The utility grid will be unable to regulate the frequency and voltage of the independently operating DG units during Islanding. After that, it can cause severe issues with power quality, extensive damage to equipment, and even safety risks for utility operation staff. So, it is important to spot islanding as soon as possible [4, 5].

Common islanding detection techniques include communication-based, passive, and active approaches [6]. While the non-detection zone (NDZ) of communication-based technologies is small, having no negative effects on the quality of power supplied these approaches are more expensive and hard to operate [7]. Both passive and active methods have been developed to this point, but the passive islanding recognition strategies rely on quantifying system parameters (like variation in the frequency, voltage, phase angle, and total harmonic distortions) that lead the inverter to control and modify the output power to get categorical conditions during islanding mode [8]. The most common passive islanding detection methods assess the PCC current and voltage from the DG to ascertain the islanding state. These methods include phase jump detection, over/under voltage protection, and over/under frequency protection [9]. When the system is isolated, there is a drastic notable variation in PCC parameters. When the load and generation in an islanded system are very similar, passive detection methods have trouble picking up on islanding [10]. The thresholds for these variables also require careful consideration. A false DG trip can occur if the threshold is too low, while failure to detect islanding can occur if the threshold is too high [11, 12]. To determine if islanding has occurred, active approaches inject perturbations or harmonics into specific DG parameters. By producing a continual tendency to transform the frequency during islanding, the active frequency drift [13], slip-mode frequency shift [14], and Sandia frequency shift methods [15] are three classical active approaches. However, active approaches are more susceptible to weak NDZs, and the existence of perturbations during healthy operations will compromise power quality and dependability. Some active methods also have trouble staying in sync when used in a hybrid setting [16, 17]. Passive detection methods typically employ time domain analysis. Although pure derivative in time domain analysis has been used in previous works on passive detection techniques to magnify the ripple, its actual implementation as a controller is brittle [18, 19].

In this article, we have implemented a passive islanding recognition strategy using time domain analysis in a hybrid distributed generating system which detects islanding conditions during critical conditions such as load power matches the DG power. In order to smooth out the islanding detection without affecting the power quality, the suggested method expands the window size beyond the threshold limit used to generate a bigger variation in the waveform during grid-connected and islanding modes of operations. Therefore, it produces results regardless of the quantity, size, or kind of DG linked to the electric grid.

The paper is organized as follows: Section 2 presents the hybrid distributed generation test system. Section 3 provides an overview of the islanding detection method under consideration. Section 4 discusses the results and the suggested approach. Finally, Section 5 presents the concluding remarks.

## 2. Hybrid DG system

The power produced by the hybrid network is transmitted to the utility system side in grid-connected hybrid PMSG-PV systems via a series of electrical elements that transform the DC voltage into the AC voltage [20]. Figure 1 shows the simplified schematic of a Hybrid system (PV and Wind), DC-DC boosting

**Table 1.** Simulink Model Parameters.

Parameter	Value
PV capacity	100 kW
PMSG capacity	7 kW
Load power	107 kW
Quality factor of load	1
Resonant frequency	60 Hz
DC link voltage	500 V
Inverter switching frequency	33*60 Hz

element and 3-phase inverter all linked to the utility system via a step-up transformer. Simulink model parameters are listed in Table 1.

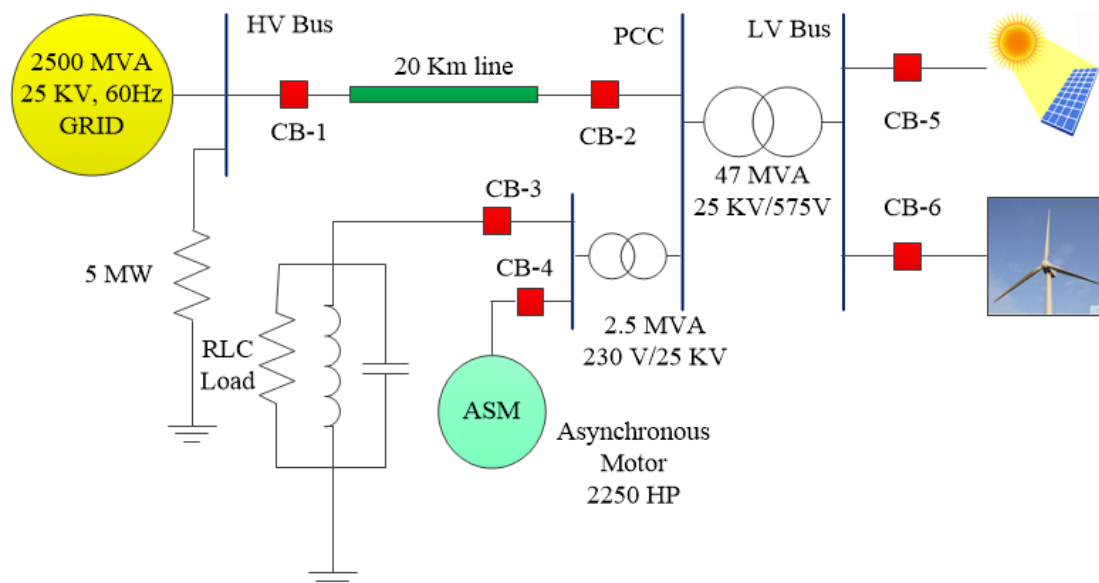


**Figure 1.** Combined solar and wind energy system depicted in a single line diagram.

### 2.1. Incremental conductance algorithm in PV System

This algorithm compares the incremental conductance, which is the change of current  $\Delta i$  divided by the change of voltage  $\Delta v$ , to the instantaneous conductance, which is the current ( $i$ ) divided by the voltage ( $v$ ) to get the maximum power point (MPP). This technique employs a graphical strategy that expands upon the PV module as an illustrative  $P - V$  curve [21]. The operational point of the PV system is finished with the use of equations in the incremental conductance approach. When the PV system is working at the MPP, Equation (1) holds true; when the PV system is working on the left side of the MPP, Equation (2) holds true; and when the PV system is working on the right side of the MPP, Equation (3) holds true [22],

$$\Delta i / \Delta v = i / v, \tag{1}$$

$$\Delta i / \Delta v > -i / v, \tag{2}$$

$$\Delta i / \Delta v < -i / v. \tag{3}$$

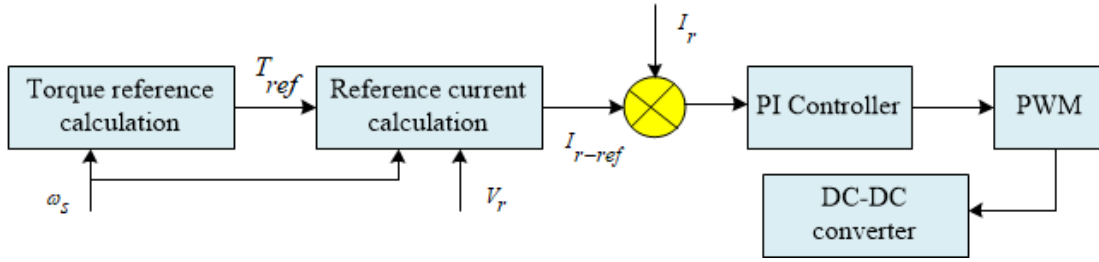


**Figure 2.** Control strategy for optimum torque control.

The approach relies on the statement that the gradient of the P-V curve becomes close to zero at the MPP. The conditions to achieve the MPP in this algorithm are defined as,

$$dp/dv = 0, \quad (4)$$

$$i + v(di/dv) = 0. \quad (5)$$

Pulse-width modulation (PWM) is recognized to regulate the yield voltage of a DC boost converter by varying the switching frequency of the converter during operation. The boost converter input voltage signal is related to its output voltage via

$$v_{out} = -v_{in}(d/1 - d), \quad (6)$$

where  $d$  represents the duty cycle determined by the maximum power point tracking (MPPT) algorithm. MPP's superior efficiency, proximity, and rapid tracking in comparison to alternative algorithms make it the algorithm of choice.

## 2.2. Algorithm based on optimum torque controlling in wind-PMSG System

Due to its stability and lack of oscillation, optimum torque control performs exceptionally well as a component of maximum power extraction. The DC-DC converter would be integrated using this method [23]. The available produced power from PMSG wind system can be mathematically expressed as,

$$P_{m-opt} = 0.5\rho AC_{p-opt}(\omega_{m-opt}R/\lambda_{opt})^3, \quad (7)$$

$$K_{opt} = 0.5AC_{p-opt}(R/\lambda_{opt})^3, \quad (8)$$

$$\omega_{m-opt} = (\lambda_{opt}/R) u_w = K_{\omega} u_w. \quad (9)$$

The required torque can be expressed as

$$T_{m-opt} = K_{opt}(\omega_{m-opt})^2. \quad (10)$$

To get the most power out of a wind machine whose speed changes, the following steps are part of the algorithm shown in Figure 2: (i) Figure out the optimal power you want to reach. (ii) Measure generator speed  $\omega_m$  (iii) Using  $\omega_m$  and optimum torque, figure out the reference torque (iv). With the rectifier output voltage  $V_r$  (v), this torque base is used to figure out the DC current reference value. Compare the DC reference current with the calculated rectifier yield current, which is sent to the PI controllers. The PWM controller then makes the switching pulses that control the duty cycle of the entire system [24]. Optimal power based on the speed of the generator keeps the generator in line.

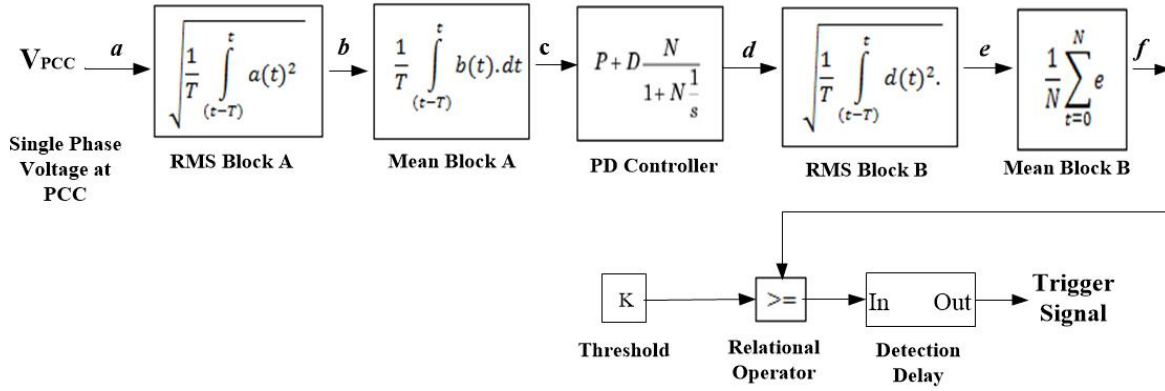


Figure 3. Block diagram for modified islanding detection technique.

### 3. Proposed islanding detection method

The mathematical formula for the islanding voltage is given by,

$$V_{isl} = V_g \sqrt{P_{inv} / P_{load}}, \quad (11)$$

where  $V_{isl}$  is the voltage measured at PCC after islanding,  $V_g$  is the voltage measured at the grid side. When there is no power difference  $P_{inv} = P_{load}$  and  $V_{isl} = V_g$ , this is considered the worst case. So, passive islanding identification methods do not work to find islanding. To get around these problems, a modified passive islanding recognition strategy using time domain spectral analysis is made. This technique looks at the ripples in the instantaneous yield voltage signal of the inverter at PCC. Figure 3 shows a block diagram of the new islanding identification method.

The single-phase voltage from PCC goes through RMS block A, and then the signal goes to mean block A to filter out frequencies higher than 60 Hz, and the output of the mean block goes through a PD controller with a derivative filter that amplifies the ripples in the filtered signal. The signal is then sent to RMS block B, which works at FRMS = 6Hz to smooth out the ripples in the signal amplified by the PD controller and get rid of the DC component. Mean block B works at  $f_{mean}$  because the output of RMS block B is filtered at 6Hz. The signal from the middle block B is compared to a level that has already been set. If it goes over the barrier for a certain amount of time, this is called "islanding". The amplitude of mean block B is compared to a predetermined cutoff ( $k$ ). If the amplitude of mean block B is greater than ( $k$ ) for a predetermined amount of time ( $t_k$ ), islanding is found when the triggering parameter is high (level 1) and low (level 0) otherwise as

$$\text{Trigger} = \begin{cases} 1 & \text{if } - \text{magnitude} \geq k, \Delta t \geq k_t \\ 0 & \text{otherwise} \end{cases}. \quad (12)$$

A MATLAB/Simulink model was used to construct the suggested islanding estimation technique as shown in Figure 4. The simulation parameters are shown in Table 1. The system comprises a hybrid Permanent Magnet Synchronous Generator-Photovoltaic (PMSG-PV) unit, which is grid-connected and operates at a fundamental frequency of 60 Hz. The PV (1000W/m<sup>2</sup> irradiance at 25°C) gets the most power by using an MPPT algorithm based on the incremental conductance method to control the duty cycle of the DC-DC converter [25]. In order to get the most power out of the changing wind, the wind turbine engine has to work at different speeds. This needs a complex control approach, as Optimum torque tracking is used to get the most out of the wind energy. By connecting an MPPT controller with optimal torque tracking to a DC-DC converter, the DC voltage from the wind can be matched up with the DC

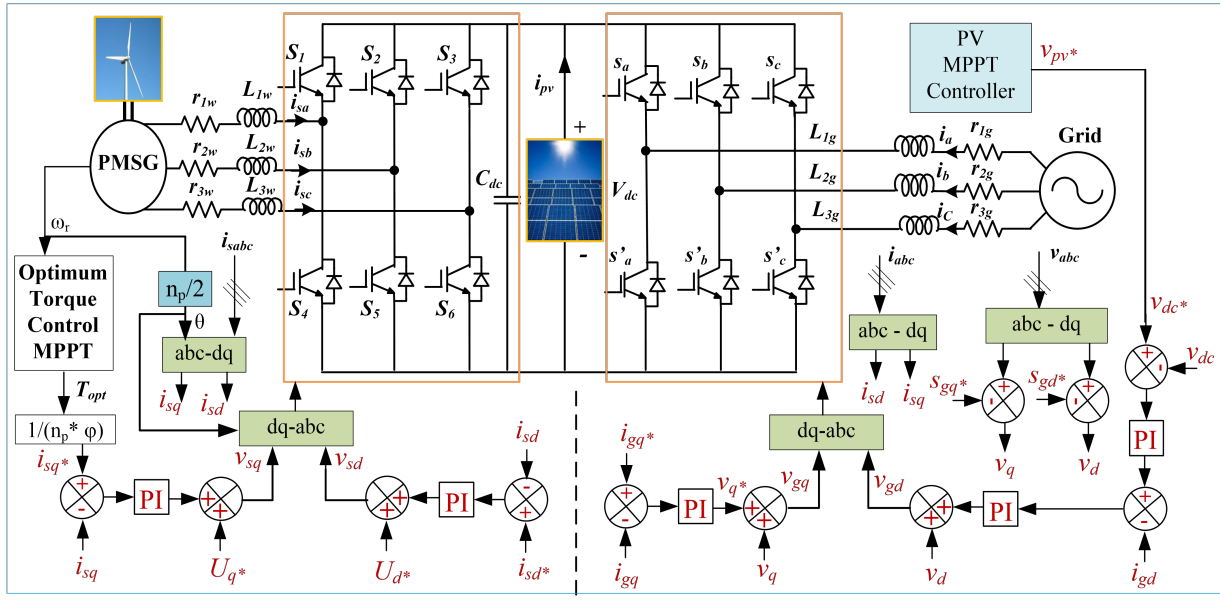


**Figure 4.** Simulation diagram of the hybrid (PV and Wind) system.

voltage from the DC link. The 3-phase inverter uses the DC link power to turn DC into AC. The control sequence for generating inverter pulses in the Voltage Source Converter (VSC) control system involves the following steps: (i) Generation of a current reference  $I_{dref}$  by comparing the measured hybrid DC link voltage to the DC reference voltage, while  $I_{qref}$  remains at zero to maintain a power factor of 1. (ii) Measurement of voltage and current on the grid side, followed by conversion into  $I_d - I_q$  components. (iii) The inverter's reference voltage is determined by the current regulator based on the current reference  $I_{dref}$ . These steps enable the generation of switching signals for the inverter. To mitigate harmonics induced by the high switching frequencies of the inverter, a series RL filter and a capacitor bank are employed in tandem. Post-filtering, the inverter's output voltage is adjusted to 260V (RMS). The inverter is connected to a step-up transformer, which in turn interfaces with the primary utility at the Point of Common Coupling (PCC). Additionally, it is connected to an RLC load with a quality factor of 1. The utility grid is represented as a 25 kV equivalent transmission system with a short-circuit capacity of 2500 MVA and an  $X/R$  ratio of 7.

## 4. Results and Discussion

### 4.1. Waveforms Taken at Various Points in the Islanding Detection Process

Figure 5 shows the waveforms at each output of all the stages of the proposed islanding detection method. Figure 5(a) displays the voltage waveform in a single phase at the PCC. The root mean square RMS value of  $V_{pcc}$  is shown in Figure 5(b). The RMS block figures out the true RMS value of the input signal over one turn of the fundamental frequency, which is set to 60 Hz as,

$$\text{RMS}(f(t)) = \sqrt{1/T \int_{t-T}^T f(t)^2 dt}, \quad (13)$$

where  $f(t)$  is the input signal and  $T$  is  $1/60$ . The output of Mean block A (Figure 5) is modeled as,

$$\text{Mean}(f(t)) = 1/T \int_{t-T}^T f(t)dt. \tag{14}$$

The average of one cycle of the fundamental frequency, which is set to 60 Hz, is used to figure out the mean number. Use the PD controller with filter derivative to get the pattern in Figure 5(d). This will make the changes in Figure 5(c) bigger. For better performance, the output of the PD controller is sent to the RMS block B with a fundamental frequency of 6 Hz and a sampling time of 10 sec, as shown in Figure 5(e). The output of the RMS block B is then sent to the Mean block B with a fundamental frequency of 6 Hz and a sampling time of 10 sec. Lastly, any frequency component over  $f_{mean}$  in Figure 5(e) is taken out to get the pattern in Figure 5(f), which shows islanding detection.

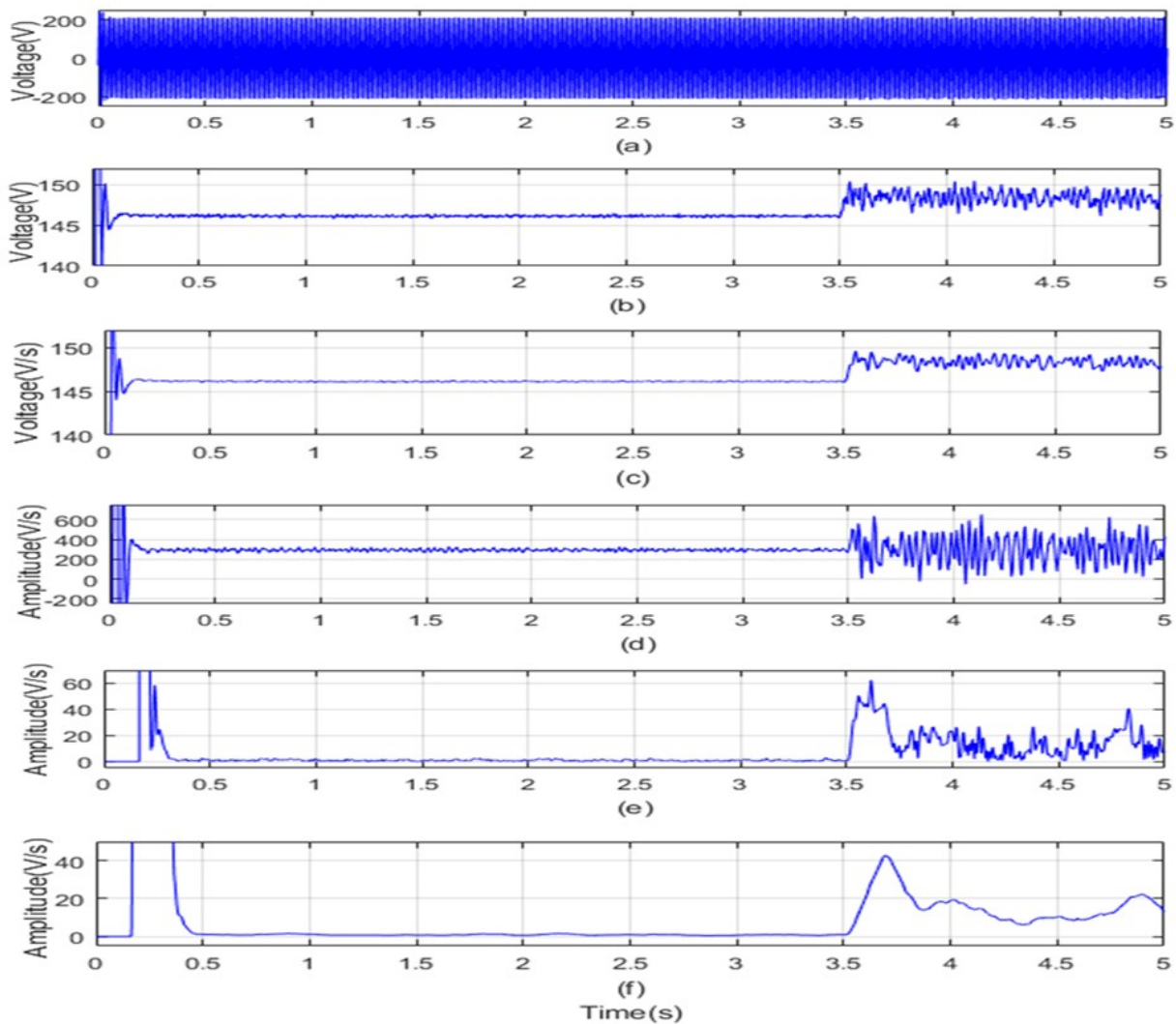


**Figure 5.** Output waveforms of the stage (a) single phase voltage at PCC (b) RMS block A (c) Mean block (d) PD controller (e) RMS block B (f) Mean block B (Islanding Detection Waveform).

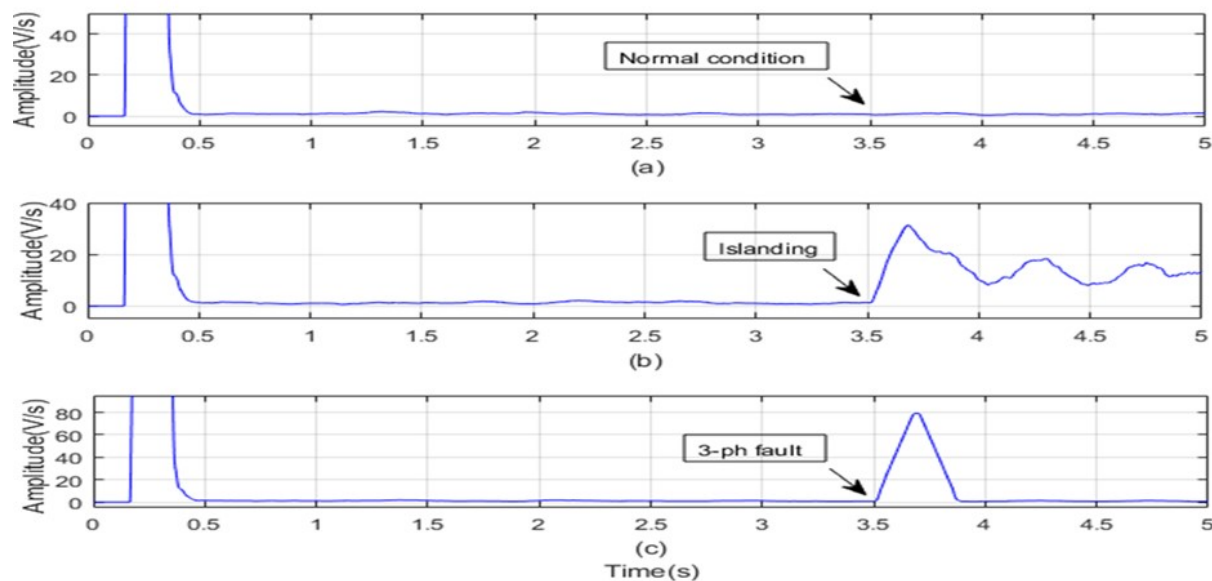


**Figure 6.** Islanding recognition waveform in (a) Grid-connected (b) Islanding (c) 3-ph short-circuit fault

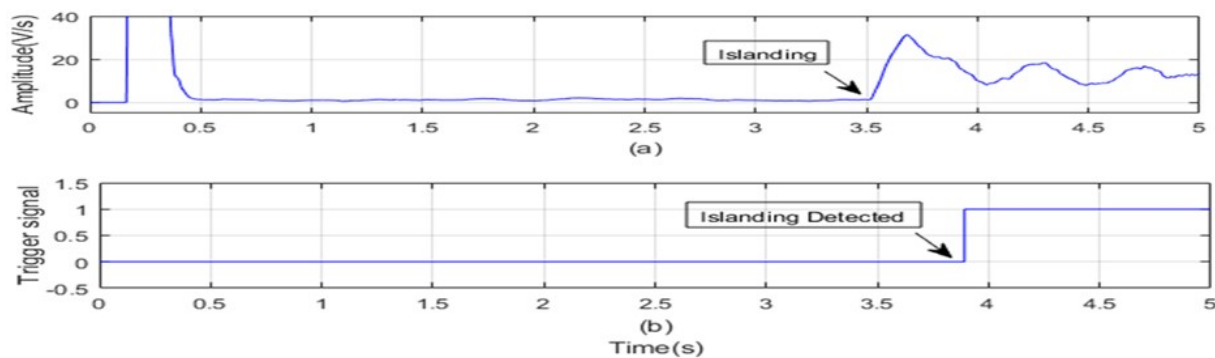


**Figure 7.** Zero power mismatch case (a) Islanding detection waveform (b) Triggering waveform.

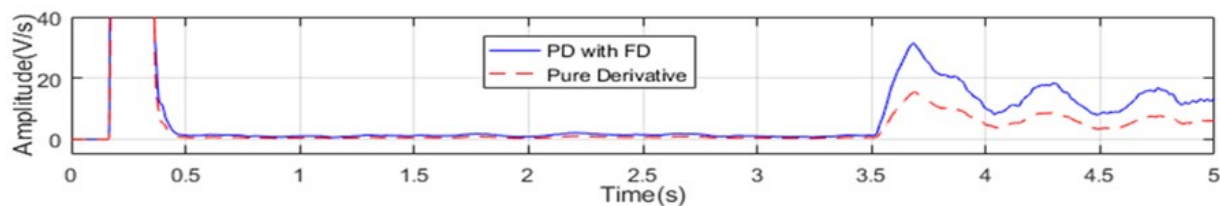
#### 4.2. Islanding Detection Waveform in Various Conditions

Figure 6 focuses Islanding estimation waveform variations in a grid integrated state, an islanding state (Figure 6(b)), and a non-islanding state (Figure 6(c)). From Figure 6(a) and 6(b), it is clear that the islanding detection pattern is always different before and after islanding in the scenario where there is no islanding, the waveform that is illustrated in Figure 6(c) has a peak that very quickly achieves its maximum value. In the final phase, a time delay is implemented so that there will not be any false trips in situations where there is no landing.

#### 4.3. Detection of Islanding in the Event of a Zero-Power Mismatches

The waveform and trigger signal for islanding identification are depicted for a scenario in Figure 7 in which there is no power mismatch  $P_{inv} = P_{load}$ . Because the islanding recognition waveform is lower than the set value that has been specified, the trigger signal does not become active until after islanding has occurred. On the other hand, once islanding has occurred, the islanding detection waveform amplitude must have been higher than a certain set for a predetermined amount of time for the trigger signal to become high (level 1). As seen in Figure 7(b), islanding occurs approximately 0.35 seconds after the grid is initially





**Figure 8.** Comparison between pure Derivative and PD controller with filter derivative.

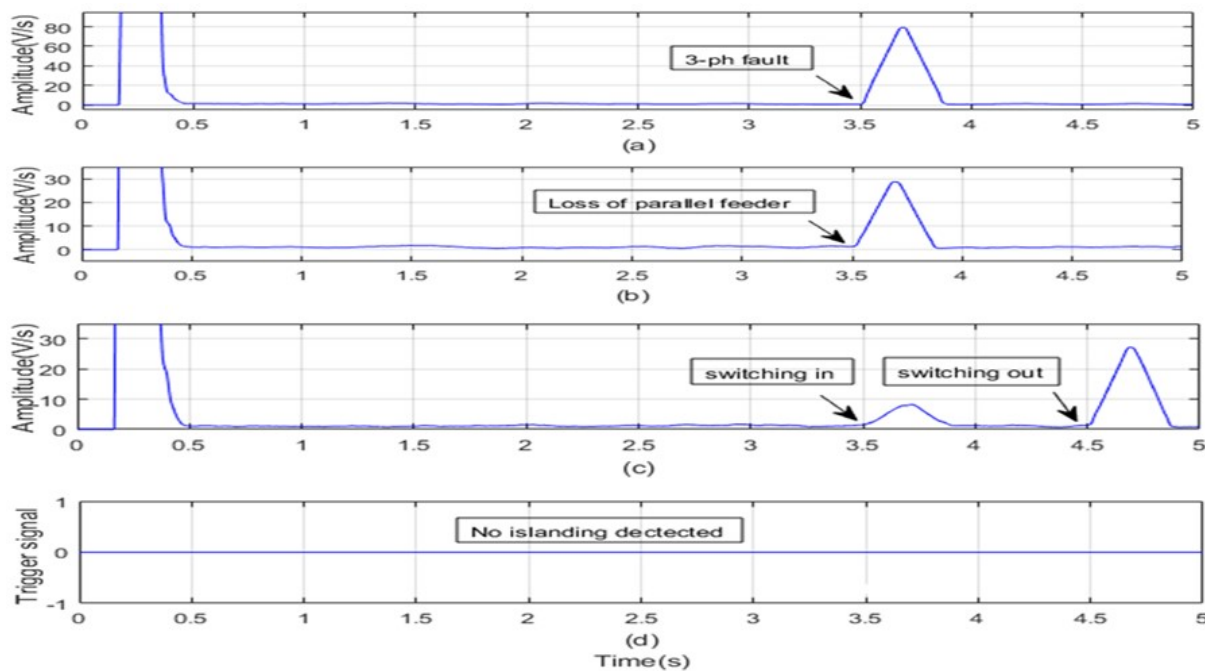


**Figure 9.** Non-islanding waveform (a) 3-ph short circuit (b) Loss of parallel feeder (c) load switching (d) trigger signal.

opened. The islanding is confirmed at approximately 0.39 seconds, which means the proposed method detected the zero power balanced islanding within 40 ms. The proposed method was also tested for different islanding cases with various power mismatches and achieved the best results in islanding detection against the reported in the literature. Various non-islanding cases are also simulated with the proposed method in the next sections.

#### 4.4. Changing Window Size using PD Controller

According to the literature, the pure derivative is what’s utilized to make the ripple bigger. However, it is difficult to employ pure derivative controllers in the real world. In order to expand the window size and provide a more bearable level of disparity among the islanding and grid integrated levels, proportional-derivative (PD) controllers with filtered derivatives are utilized. As a result, the threshold level will be raised, which will result in the islanding recognition signal being more uniform, as depicted in Figure 8.

**Table 2.** Comparison of proposed method with literature.

Reference	Parameter/Method	Type of DG used	Detection Time	NDZ
[26]	Voltage, frequency	PV	3 cycles	Small
[27]	Voltage, active power	PV, wind	50 ms	Small
[28]	Voltage, ANN	PV	20 ms	Small
[29]	Voltage	PV	160 ms	Small
[30]	Frequency, Impedence	PV	130 ms	Small
Proposed method	Voltage	PV, Wind	40 ms	Zero

#### 4.5. Non-Islanding Cases

The islanding sensor may go off even if there is not an island present because of failures such as short circuits, loss of parallel feeder, and load switching, among other potential causes. Figure 9 displays the outcomes that were achieved by modeling these different scenarios. Because the waveform in each of the following examples contains a peak that disappears rather rapidly, a time delay and a threshold are applied in order to prevent false tripping. The trigger signal is essential in every one of the scenarios presented in Figure 9(d). The proposed method is compared with the literature in terms of the type of parameter used, NDZ, and power quality issues are presented in Table 2.

## 5. Conclusion

An innovative islanding recognition method for a hybrid distributed generating network was demonstrated in this body of work. The method that has been suggested is distinct from both passive and active islanding detection in the sense that it does not have an NDZ. When attempting to identify islanding using this technique, ripples in the RMS voltage measured at the PCC are investigated. This takes roughly 0.4 seconds in the time domain analysis, and it is proven for other non-islanding scenarios, such as fault condition, loss of parallel feeder, load switching, etc., by setting a predetermined threshold for a particular length of delay time. Other non-islanding cases include: fault condition, loss of parallel feeder, load switching, etc. Additionally, it demonstrates how the smoothness of the islanding detection waveform may be improved by raising both the window size and the cutoff limit.

## Acknowledgments

The authors would like to thank VELS Institute of Science, Technology & Advanced Studies, Chennai for supporting this research work.

**Funding:** This research received no external funding.

### Author contributions:

Conceptualization, S. V. R. and C. R. R; Methodology, S. V. R; Software, S. V. R; Validation, C. R. R, T. R. P. and B. N. R; Formal Analysis, C. R. R; Investigation, S. V. R; Resources, S. V. R; Data Curation, S. V. R; Writing – Original Draft Preparation, S. V. R; Writing – Review & Editing, C. R. R; Visualization, B. N. R; Supervision, T. R. P and C. R. R; Project Administration, B. N. R; Funding Acquisition, T. R. P.

**Disclosure statement:** The authors declare no conflict of interest.

## References

- [1] Sareddy Venkata Rami Reddy, TR Premila, Ch Rami Reddy, Muhammad Majid Gulzar, and Muhammad Khalid. A new variational mode decomposition-based passive islanding detection strategy for hybrid distributed renewable generations. *Arabian Journal for Science and Engineering*, pages 1–9, 2023.
- [2] Ch Rami Reddy, Obbu Chandra Sekhar, B Pangedaiah, Khalid A Khan, and Muhammad Khalid. Passive island detection method based on positive sequence components for grid-connected solar–wind hybrid distributed generation system. *Electric Power Components and Systems*, pages 1–16, 2023.
- [3] Sareddy Venkata Rami Reddy, TR Premila, Ch Rami Reddy, Mohammed A. Alharbi, and Basem Alamri. Passive island detection method based on sequence impedance component and load-shedding implementation. *Energies*, 16(16):5880, 2023.
- [4] SA Saleh, AS Aljankawey, Ryan Meng, J Meng, L Chang, and CP Diduch. Apparent power-based anti-islanding protection for distributed cogeneration systems. *IEEE Transactions on Industry Applications*, 52(1):83–98, 2015.
- [5] Sheetal Chandak, Manohar Mishra, and Pravat Kumar Rout. Hybrid islanding detection with optimum feature selection and minimum ndz. *International Transactions on Electrical Energy Systems*, 28(10):e2602, 2018.
- [6] Mohsen Bakhshi, Reza Noroozian, and Gevork B Gharehpetian. Novel islanding detection method for multiple dgs based on forced helmholtz oscillator. *IEEE Transactions on Smart Grid*, 9(6):6448–6460, 2017.
- [7] P Ramya, K Sahithya, T Vamsi, and B Pangedaiah. Improvement in the power quality by using dynamic voltage restorer. In *2022 IEEE 2nd Mysore Sub Section International Conference (MysuruCon)*, pages 1–6. IEEE, 2022.
- [8] Pangedaiah Bezawada, Pedda Obulesu Yeddula, and Venkata Reddy Kota. A new time domain passive islanding detection algorithm for hybrid distributed generation systems. *International Transactions on Electrical Energy Systems*, 30(12):e12632, 2020.
- [9] SK Arshiyarveen, V Jithendra Teja, M Naveen Kumar, and B Pangedaiah. Power quality improvement in dfig wind power system by fuzzy controlled upqc. In *2022 IEEE 2nd Mysore Sub Section International Conference (MysuruCon)*, pages 1–5. IEEE, 2022.
- [10] Ch Rami Reddy and K Harinadha Reddy. A deep cnn approach for islanding detection of integrated dg with time series data and scalogram. *Soft Computing*, 27(8):4943–4951, 2023.
- [11] Bangar Raju Lingampalli, Subba Rao Kotamraju, M Kiran Kumar, Ch Rami Reddy, Mukesh Pushkarna, Mohit Bajaj, Hossam Kotb, Sadam Alphonse, et al. Integrated microgrid islanding detection with phase angle difference for reduced nondetection zone. *International Journal of Energy Research*, 2023, 2023.
- [12] Ch Rami Reddy, M Kondalu, S Ravindra, G Srinivasa Rao, B Srikanth Goud, and A Narasimha Reddy. Convolution neural network and continuous wavelet transform-based islanding detection of integrated dg with phase angle between voltage and current. In *Smart Energy and Advancement in Power Technologies: Select Proceedings of ICSEAPT 2021 Volume 1*, pages 177–193. Springer, 2022.
- [13] Basanta K Panigrahi, Anshuman Bhuyan, Jyoti Shukla, Prakash K Ray, and Subhendu Pati. A comprehensive review on intelligent islanding detection techniques for renewable energy integrated power system. *International Journal of Energy Research*, 45(10):14085–14116, 2021.
- [14] Soham Dutta, Pradip Kumar Sadhu, M Jaya Bharata Reddy, and Dusmanta Kumar Mohanta. Shifting of research trends in islanding detection method—a comprehensive survey. *Protection and Control of Modern Power Systems*, 3:1–20, 2018.
- [15] Ashish Shrestha, Roshan Kattel, Manish Dachhepatic, Bijen Mali, Rajiv Thapa, Ajay Singh, Diwakar Bista, Brijesh Adhikary, Antonis Papadakis, and Ramesh Kumar Maskey. Comparative study of different approaches for islanding detection of distributed generation systems. *Applied System Innovation*, 2(3):25, 2019.

- [16] S Govinda Raju, K Harinadha Reddy, and Ch Rami Reddy. Islanding detection parameters for integrated distributed generation. *Recent Advances in Electrical & Electronic Engineering (Formerly Recent Patents on Electrical & Electronic Engineering)*, 14(2):131–143, 2021.
- [17] J Rajesh Reddy, Alagappan Pandian, R Dhanasekharan, Ch Rami Reddy, B Prasanna Lakshmi, and B Neelima Devi. Islanding detection of integrated distributed generation with advanced controller. *Indonesian Journal of Electrical Engineering and Computer Science*, 17(3):1626–1631, 2020.
- [18] Ch Rami Reddy and K Harinadha Reddy. Islanding detection techniques for grid integrated dg: a review. *International journal of renewable energy research*, 153(2):960, 2019.
- [19] Ch Rami Reddy and K Harinadha Reddy. A passive islanding detection method for neutral point clamped multilevel inverter based distributed generation using rate of change of frequency analysis. *International journal of electrical and computer engineering*, 8(4):1967, 2018.
- [20] PVV Satyanarayana, A Radhika, Ch Rami Reddy, B Pangedaiah, Luigi Martirano, Andrea Massaccesi, Aymen Flah, and Michał Jasiński. Combined dc-link fed parallel-vsi-based dstatcom for power quality improvement of a solar dg integrated system. *Electronics*, 12(3):505, 2023.
- [21] B Pangedaiah, PL Santosh Kumar Reddy, YP Obulesu, Venkata Reddy Kota, and Mamdouh L Alghaythi. A robust passive islanding detection technique with zero-non-detection zone for inverter-interfaced distributed generation. *IEEE Access*, 10:96296–96306, 2022.
- [22] Rami Reddy, G Rami Reddy, B Srikanth Goud, N Rajeswaran, and Narendra Kumar. Passive islanding detection methods for integrated distributed generation system. *Journal of Power Technologies*, 101(3), 2021.
- [23] Ch Rami Reddy, K Harinadha Reddy, B Srikanth Goud, and B Pakkiraiah. A deep learning approach for islanding detection of integrated dg with cwt and cnn. In *2021 International Conference on Sustainable Energy and Future Electric Transportation (SEFET)*, pages 1–7. IEEE, 2021.
- [24] Ali Rostami and Navid Rezaei. A multi-feature-based passive islanding detection scheme for synchronous-machine-based distributed generation. *International Transactions on Electrical Energy Systems*, 30(11):e12586, 2020.
- [25] B Pangedaiah, YP Obulesu, and Venkata Reddy Kota. A new architecture topology for back to back grid-connected hybrid wind and pv system. *Journal of Electrical Engineering & Technology*, 16:1457–1467, 2021.
- [26] Hamdan Alosaimi, Hadhlul Aladhyani, and Subhashish Bhattacharya. Pv system control as statcom with svm-based islanding detection. In *2023 IEEE Power and Energy Conference at Illinois (PECI)*, pages 1–7. IEEE, 2023.
- [27] B Hariprasad, P Bharat Kumar, P Sujatha, and G Sreenivasan. Island detection in inverter based distributed generation using a hybrid method. In *2022 Second International Conference on Artificial Intelligence and Smart Energy (ICAIS)*, pages 1702–1707. IEEE, 2022.
- [28] Ashutosh Mohanty and Bidyadhar Rout. Island detection based on voltage ratio and artificial neural network for inverter-based distributed generation. In *2022 International Conference on Intelligent Controller and Computing for Smart Power (ICICCSP)*, pages 1–6. IEEE, 2022.
- [29] Subhradip Mondal, Pritam Kumar Gayen, and Dattatraya N Gaonkar. A hybrid islanding detection method based on lissajous pattern having robust performance under various power quality scenarios. *IEEE Systems Journal*, 2022.
- [30] Tianling Shi, Hongyi Chen, Boxin Liu, Shiyuan Fan, Fei Wang, Xin Xiang, Huan Yang, and Wuhua Li. Detecting speed improvement and system stability enhancement for dc microgrids islanding detection based on impedance characteristic analysis. *IEEE Transactions on Power Electronics*, 38(3):3785–3802, 2022.